ACS OMEGA

http://pubs.acs.org/journal/acsodf

Article

Molecular Recognition of the Self-Assembly Mechanism of Glycosyl Amino Acetate-Based Hydrogels

Yi Zhou, Jiamei Liu, Hui Li, Heng Zhang,* Zhaoyong Guan,* and Yanyan Jiang*

Cite This: *ACS Omega* 2021, 6, 21801−21808

Read Online

ACCESS | Metrics & More | Article Recommendations | Supporting Information

ABSTRACT: The self-assembly of supramolecular hydrogels has attracted the attention of many researchers, and it also has a broad application prospect in biomedical fields. However, there are few studies on the intrinsic mechanism of molecular self-assembly of hydrogels. In this paper, the self-assembly process of glycolipid-based hydrogels is studied by combining quantum chemistry calculation and molecular dynamics simulation. Using quantum chemistry calculation, the stable stacking mode of gelator dimers was explored. Then, by varying the water content in the gelation system, three different morphologies of hydrogels after self-assembly were observed on the nanoscale. When the water content is low, the molecular chains were entangled with each other to form a three-dimensional network structure. When the water content is moderate, the system had obvious stratification, forming the typical structure of "gel−water−gel". The gelators can only form small micelle-like agglomerations when the water content is too high. According to the analysis of the interaction between gelators and that between gelators and water molecules, combined with the study of the radial distribution function and hydrogen bonding, it is determined that the hydrogen bonds formed between gel molecules are the main driving force of the gelation process. Our work is of guiding significance for further exploration of the formation mechanism of a hydrogel and developing its application in other fields.

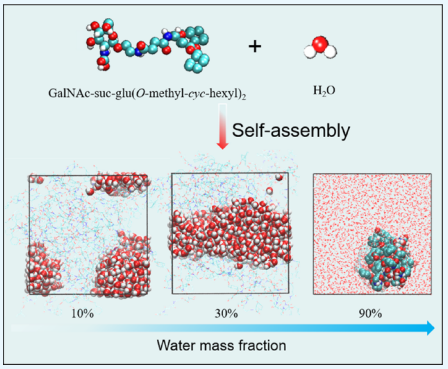

1. INTRODUCTION

In nature, molecular self-assembly is ubiquitous,[1] especially for biological macromolecules such as DNA and proteins, which is more common. However, self-assembly of small molecules in water (or organic solvents) also has far-reaching implications from basic science to practical applications.[2] Many researchers have studied the self-assembly behavior of small molecules extensively and deeply. Supramolecular hydrogels are usual structures formed by the self-assembly of small molecules. Different from traditional hydrogels, which are connected together by covalent bonds to form a three-dimensional network structure,[3,4] the formation of supramolecular hydrogels depends on the weak interaction between small molecules, including hydrogen bonding, electrostatic interaction, van der Waals,[5,6] and so forth. This subtle but fundamental difference makes the molecular arrangement of supramolecular hydrogel monomers orderly and results in a dynamic and reversible molecular assembly.[7] Therefore, supramolecular hydrogels are more sensitive to environmental changes. When pH, temperature, ionic strength, and other changes occur,[8] their assembled structures and intermolecular interactions will be significantly affected. Based on this characteristic, researchers have used supramolecular hydrogels to achieve controlled drug delivery,[9] tissue engineering,[10] antibacterial activity,[11] and other applications in the biomedical field.

Hamachi et al. accidently discovered that *N*-acetyl-galactosamine-appended amino acid ester (GalNAcaa) can effectively gel a variety of organic solvents when they were performing solid-phase synthesis of artificial glycolipids.[12] Even more surprising is that some GalNAc-aa derivatives exhibit excellent hydrogelation capability. Based on this discovery, they constructed a library of glycolipid mimics through chemical synthesis and discovered some hydrogelator agents through screening.[13] One typical example of the many derivatives of GalNAcaa is GalNAc-suc-glu(*O*-methyl-*cyc*-hexyl)$_2$, which has excellent hydrogelation ability and can gel water at a lower concentration.[12] Hamachi and others made reasonable chemical modifications to this hydrogel molecule to stimulate the development and application of reactive supramolecular hydrogels.[7,14] For example, the photoisomerizable C−C double bond can be combined into the molecule to form a photoresponsive hydrogel. Under ultraviolet irradiation, the molecule will exhibit cis−trans photoisomerization.[14] Therefore, supramolecular nanofibers will collapse under ultraviolet radiation and undergo microscopic gel−sol transition, which is

Received: July 5, 2021
Accepted: August 4, 2021
Published: August 13, 2021

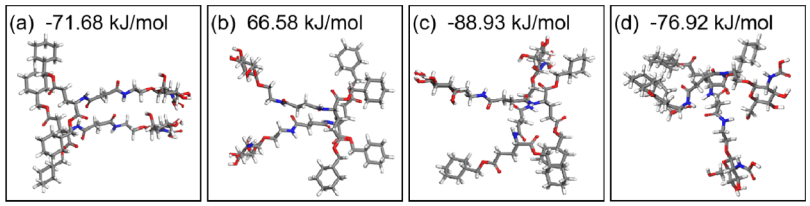

Figure 1. Optimized dimer configurations and their corresponding binding energies. (a) AA−BB parallel stacking, (b) AA−BB Y-shaped stacking, (c) AB−BA mixed stacking, and (d) AB−BA Y-shaped stacking.

expected to be applied in environmentally sensitive actuators, cell culture, and so forth.[13]

Many researchers have mainly used organic synthesis methods and various experimental characterization methods to study the structural characteristics of low-molecular weight organic/hydrogels from a macroperspective.[15] According to Hamachi et al.'s previous work, they confirmed that a developed hydrogen bond network was the key for GalNAc-suc-glu(*O*-methyl-*cyc*-hexyl)$_2$ to gelation.[12] However, at the nanometer level, the specific arrangement of the molecules and the individual atoms of the constituent molecules cannot be observed by existing characterization methods and the formation process of the hydrogel and the final assembly structure cannot be accurately described.[16] Understanding the microstructure and molecular arrangement of hydrogel molecules will help us rationally design and adjust the properties of hydrogels at a molecular level and further expand the application fields of hydrogels.[2] Molecular dynamics (MD) simulation is a computational technique that has been widely used in the simulation of hydrogels in the past few decades.[17] It is based on the classical Newtonian equation of motion to calculate the dynamic behavior of the system.[18] By calculating the force and acceleration of each atom, the motion of the molecules in the system at different times can be obtained. Data such as position and speed were obtained, so as to observe the dynamic change process of the whole system. Quantum chemistry calculation can be used to optimize the structure of organic molecules and obtain the molecular configuration with relatively stable energy for MD simulation.

Therefore, in this study, taking GalNAc-suc-glu(*O*-methyl-*cyc*-hexyl)$_2$ as an example, we used the optimized structure as the initial configuration and then, a number of systems with different water contents have been constructed. Through MD simulation, the final formation state of the system and the intermolecular relationship were observed. Arrangement methods and the main driving force for the gelation process were confirmed from a microscopic point of view to gain a deeper understanding of the self-assembly behavior of small-molecule hydrogels. We believe that this study can not only promote the understanding of the self-assembly mechanism of gels at the molecular level but also contribute to the exploration and screening of new gels and provide a theoretical basis for the design of hydrogels in the future.

2. COMPUTATIONAL METHODS

2.1. Quantum Chemistry Calculations. All the quantum chemistry calculations were carried out using the DMol3 package.[19,20] Generalized gradient approximation with Perdew−Burke−Ernzerhof parametrization was used as the exchange−correlation functional.[21] The basis set consists of the double numerical atomic orbitals augmented by polarization functions, which are comparable to Gaussian 6-31G**. In order to neglect neighboring interaction, the distance between the neighboring molecule is larger than 15 Å. The real-space global cutoff radius is chosen to be 3.7 Å. The convergence criterion on the energy and electron density is set to be 10^{-5} hartree. Geometry optimizations are performed with convergence criteria of 2×10^{-3} hartree/Å on the gradient and 5×10^{-3} Å on the displacement. The van der Waals interaction adopted the DFT (density functional theory)-D method of Grimme.[22] In this work, pseudopotential is dealt with DFT semicore pseudopots, which could give the reliable results.

In order to understand the early accumulation of hydrogels, we used DFT methods to optimize the structure of the gelator dimer.[23] According to the structure optimization of the gelator dimer, we built four different initial configurations, AA−BB and AB−BA, both of which stack in parallel or in Y-shaped configurations, respectively.[23,24] A is referred to the glycosidoid group, and B is referred to the ring structure. The binding energy of dimer configurations is calculated using the formula

$$E_a = E_{dimer} - E_{single}*2$$

in which E_{dimer} and E_{single} correspond to the total energies of the gelator dimer and the single gelator molecule.

2.2. Molecular Dynamics Simulation. In order to study the influence of water content on the formation and aggregation structure of hydrogels, a system with a water content of 10, 20, 30, 40, 50, and 90% was constructed. First, a box with a size of 5 nm × 5 nm × 5 nm was established; small molecules were randomly inserted into the box, and the steepest descent method was used to optimize the system to remove close contact and overlapping.[25] The gromos54a7 united atomic force field[26] was used for calculation, and MD simulation was implemented in Gromacs.[27] Each system performed 10 ns *NVT* simulation at 298 K and 1 atm, followed by 10 ns *NPT* simulation. After that, 200 ns MD simulation was conducted at 298 K and 1 atm equilibrium operation, and the integration step was 2.0 fs. The method used for controlling the temperature was the Berendsen thermal bath method. The cutoff radius of nonbonding interaction was set to 1.4 nm. Nonbonding interactions included Lennard-Jones potential (representing van der Waals interaction) and Coulomb potential (representing electrostatic interaction). Trajectories were collected every 5000 steps for further analysis. Visual molecular dynamics (VMD)[28] was used to observe the movement of trajectory of the system.

3. RESULTS AND DISCUSSION

Herein, the self-assembly process of GalNAc-suc-glu(*O*-methyl-*cyc*-hexyl)$_2$ hydrogels was systematically investigated using the combination of DFT calculation and MD simulation. DFT calculation results were first analyzed to understand the early accumulation of glycolipid-based hydrogels. The

https://doi.org/10.1021/acsomega.1c03510
ACS Omega 2021, 6, 21801−21808

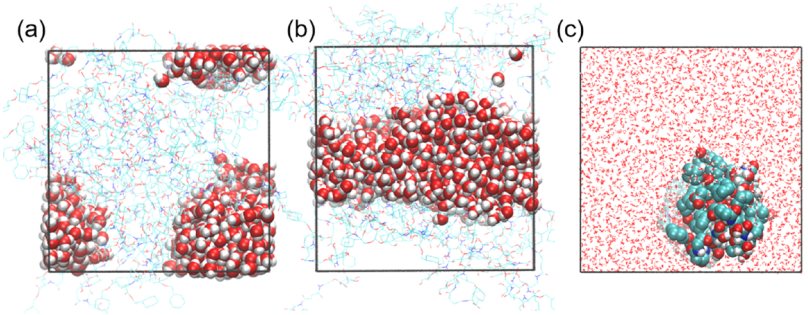

Figure 2. Snapshots of the final configuration of the system with water contents of 10, 30%, and 90%. In (a,b), the spherules are water molecules, and in (c), the spherules are hydrogel molecules.

conformation with the lowest energy after optimization of the gelator molecule is shown in Figure S1. A is referred to the glycosidoid group, and B is referred to the ring structure in the GalNAc-suc-glu(*O*-methyl-*cyc*-hexyl)$_2$ monomer. The ring structure at the tail of the gel molecule tends to be configured in parallel for maximum $\pi-\pi$ interaction, while the head glycosipids and aliphatic segments have the possibility of forming hydrogen bonds due to the presence of functional groups such as hydroxyl and amide. Therefore, we built four different initial configurations, AA−BB and AB−BA, both of which could stack in parallel and or in Y-shaped configurations, respectively. Figure 1 presents the final optimization results of the four typical dimer configurations. By comparing the binding energy of the AA−BB Y-shaped parallel stacking with those of other three stacking modes, we observe that the binding energies of the dimers in the other three stacking modes are relatively similar. It means that all three configurations are stable, where the amine group of one molecule interacts with the hydroxyl group of the other molecule to form a hydrogen bond. The binding energy shown in Figure 2b is positive, indicating that the two molecules do not easily form hydrogen bonds under this stacking mode and repel each other, so the configuration is not stable. Generally, the three configurations in Figure 1a,c,d are likely to appear in the formation and branching of the fibers in the hydrogel.

Based on the above results, MD simulations were performed to study the dynamic process of the whole gelation system. The amplitude of energy fluctuation can determine whether the simulated system reaches equilibrium. At the end of the simulation, all the systems are in balance. Taking the system with a water content of 50% as an example, the variation of the system potential energy with time is shown in the Figure S2. The results show that the system energy tends to converge at the last 50 ns of the simulation.

We constructed systems with different water mass fractions (10, 20, 30, 40, 50, and 90%) and studied their spontaneous aggregation variation with water. The final aggregation state of the system could be divided into three categories, as shown in Figure 2. When the water content is low (e.g. 10 and 20%), the hydrogel molecules are more concentrated and arranged in disorder, the molecular chains are entangled with each other to form a nanofiber network, and the water molecules distribute in the surrounding area as shown in Figure 2a. When the water content is higher (30, 40, and 50%), the system shows obvious stratification, as the "hydrogel−water−hydrogel" structure shown in Figure 2b. When simulating for a long enough time, hydrogels evenly distribute on both sides of the water layer. The hydrogel's hydrophilic groups are closer to the water molecules, but there are hydrophobic interactions between alkyl tails,[27] which tend to be far away from the distribution of water molecules. The hydrogel molecules congregate on either side of the water layer, creating a microcavity in the middle that immobilizes water molecules.[29] For the system with 90% water content, Figure 2c shows that the aggregation of gelators cannot maintain a good cross-linking and only forms small micelle-like agglomerations without forming a three-dimensional network structure. Therefore, in the following discussion, we will not take the system with 90% water content into consideration.

According to the research of Hamachi et al., the presence of a large number of hydrogen bonds in the hydrogel system is the main driving force for gelation.[30,31] Here, hydrogen bonds are defined to satisfy the following conditions:[32]

$$R_{DA} \leq 3.5\ \text{Å}, \qquad \phi \leq 30^{\circ}$$

where R_{DA} is the distance between the hydrogen bond donor and the acceptor and Φ is the angle of H−D···A.

In order to characterize the variation of hydrogen bonds with the concentration of gelators quantitatively, Figure 3 shows the number of hydrogen bonds formed between gelators and between gelators and water molecules in different water content systems. It is illustrated that with the increase in water content, the number of hydrogen bonds formed between hydrogel molecules decreases gradually and the number of hydrogen bonds formed between hydrogels and water

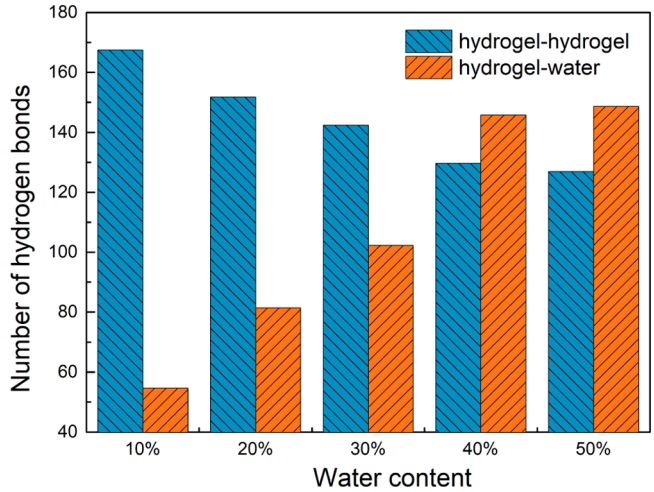

Figure 3. Hydrogen bonds in the system. Diagram of the number of hydrogen bonds in the system changing with respect to water content.

https://doi.org/10.1021/acsomega.1c03510
ACS Omega 2021, 6, 21801−21808

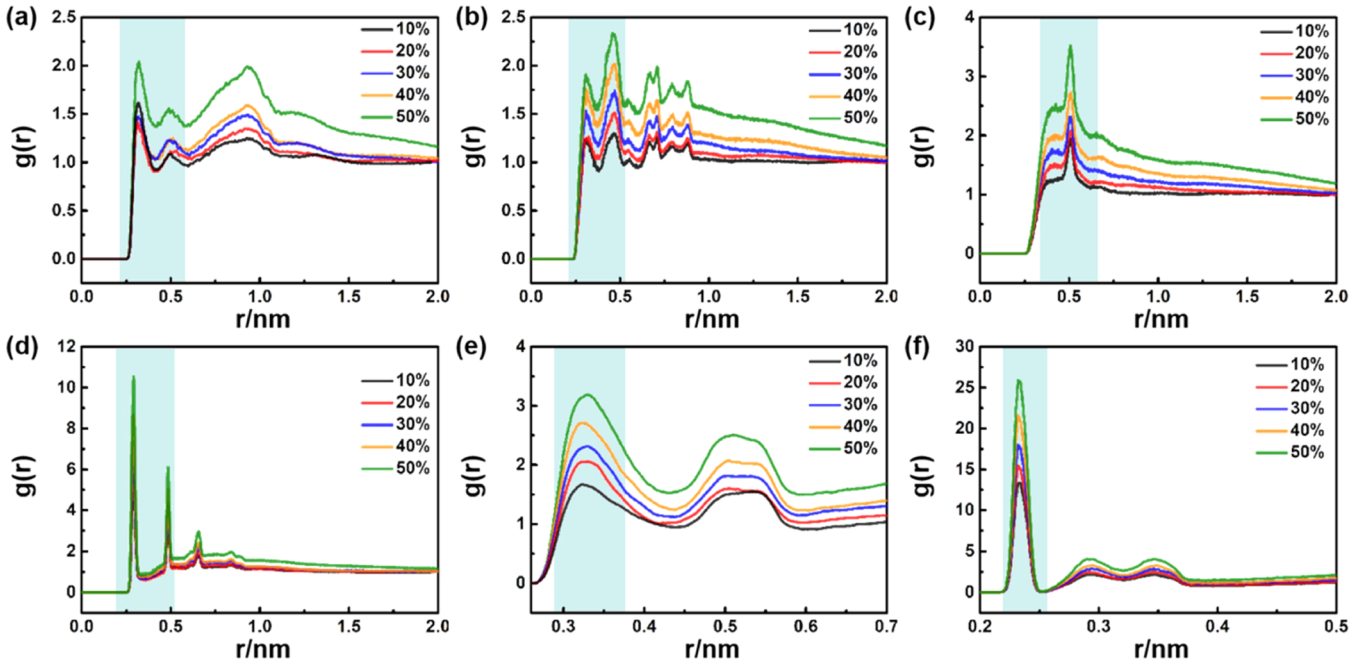

Figure 4. RDF of hydrogels. (a) Oxygen (−OH)−oxygen (−CONH) pair, (b) oxygen (−OH)−oxygen (−COO) pair, (c) oxygen (−CONH)−oxygen (−COO) pair, (d) oxygen (−OH)−nitrogen (−CONH) pair, (e) oxygen (−CONH)−nitrogen (−CONH) pair, and (f) nitrogen (−CONH) pair−oxygen (−COO) pair.

molecules increases. It is the presence of these hydrogen bonds that enables the gelators to aggregate and eventually form a stable three-dimensional network structure.

In order to understand the distribution of hydrogen bonds in the system more specifically, the radial distribution function (RDF) is used for analysis. The RDF can be interpreted as the ratio of the local density of the system to the bulk density.[33] The RDF $g(r)$ is defined by formula 1

$$g(r) = \frac{dN}{\rho 4\pi r^2} \tag{1}$$

which represents the ratio of the probability density of an atom appearing at a distance of R to the probability density of random distribution, revealing the interaction mode and nature of nonbonded atoms. In general, the peaks within 0.35 nm in $g(r)$ are mainly formed by chemical bonds and hydrogen bonds, while the peaks within 0.35−0.5 nm are mainly formed by van der Waals forces.[34]

We first studied the existence of hydrogen bonds between gelators. The nonbonding interactions among hydroxyl, carboxyl, and amide bonds and nitrogen atoms in hydrogel molecules were studied by dividing them into different groups according their features. The results are shown in Figure 4. Figure 4a shows the RDF results of the hydroxyl oxygen atom and carboxyl oxygen atom. The first peak appears at about 0.3 nm, and a smaller peak appears at 0.5 nm, indicating that the hydrogen bond is dominant between the two types of atoms and there is also a weak van der Waals force. As shown in Figure 4b, it is indicated that the main interaction between the hydroxyl oxygen atom and the oxygen atom in the amide bond is the van der Waals force with the main peak at 0.46 nm. There is a relatively high peak at about 0.31 nm, suggesting the hydrogen bonds between them. Figure 4c exhibits the RDF of the oxygen atoms in the carboxyl and amide bonds. Only one peak at 0.5 nm exists, and the interaction between them is mainly van der Waals. In Figure 4d, the oxygen atom in the hydroxyl group and the nitrogen atom in the amide bond have a sharp peak at 0.3 nm. There is a secondary peak at about 0.48 nm, indicating that the main interaction between them is the hydrogen bond, and there is also a certain van der Waals interaction. A peak at 0.33 nm exists as shown in Figure 4e. Therefore, hydrogen bonding is the main interaction between the oxygen atoms in the amide bond and the nitrogen atoms in the amide bond. Figure 4f exhibits that there is a peak at 0.23 nm, accompanying two other lower peaks at 0.29 and 0.34 nm, all of which indicate that there is a strong hydrogen bond between the nitrogen atoms in the amide bond and the oxygen atoms in the carboxyl group. Generally, systems with different water contents have RDF curves with a similar tendency. However, as the water content increases, the height of the whole curve increases. The nitrogen atoms on the amide bond have relatively high RDF peaks compared to other types of atoms, and the low abscissa position of their corresponding peak means that the probability of occurrence near the core is high. The reason is that the nitrogen atoms are connected to a hydrogen atom, which is more polar and tends to form hydrogen bonds with other atoms, thus reducing the distance between it and other atoms. Hydroxyl oxygen atoms also have hydrogen atoms attached, but they prefer to form hydrogen bonds with water molecules, so the peak value of the RDF between gel molecules is low.

The status of hydrogen bonds between the gelator and water molecules has also been investigated. As shown in Figure 3, when the water content exceeds 30%, the number of hydrogen bonds between gelators is less than that between the gelator and water molecules, which means that it is also very important to study the interaction between the hydrogel and water molecules. Hence, we have carefully analyzed the RDF between the relevant atoms in the gelator, including oxygen atoms (O2, O3, and O4) in hydroxyl groups, oxygen atoms (O8, O9, O10, O11, O12, and O13) in carboxyl groups, oxygen atoms (O6 and O7) and nitrogen atoms (N1, N2, and

https://doi.org/10.1021/acsomega.1c03510
ACS Omega 2021, 6, 21801−21808

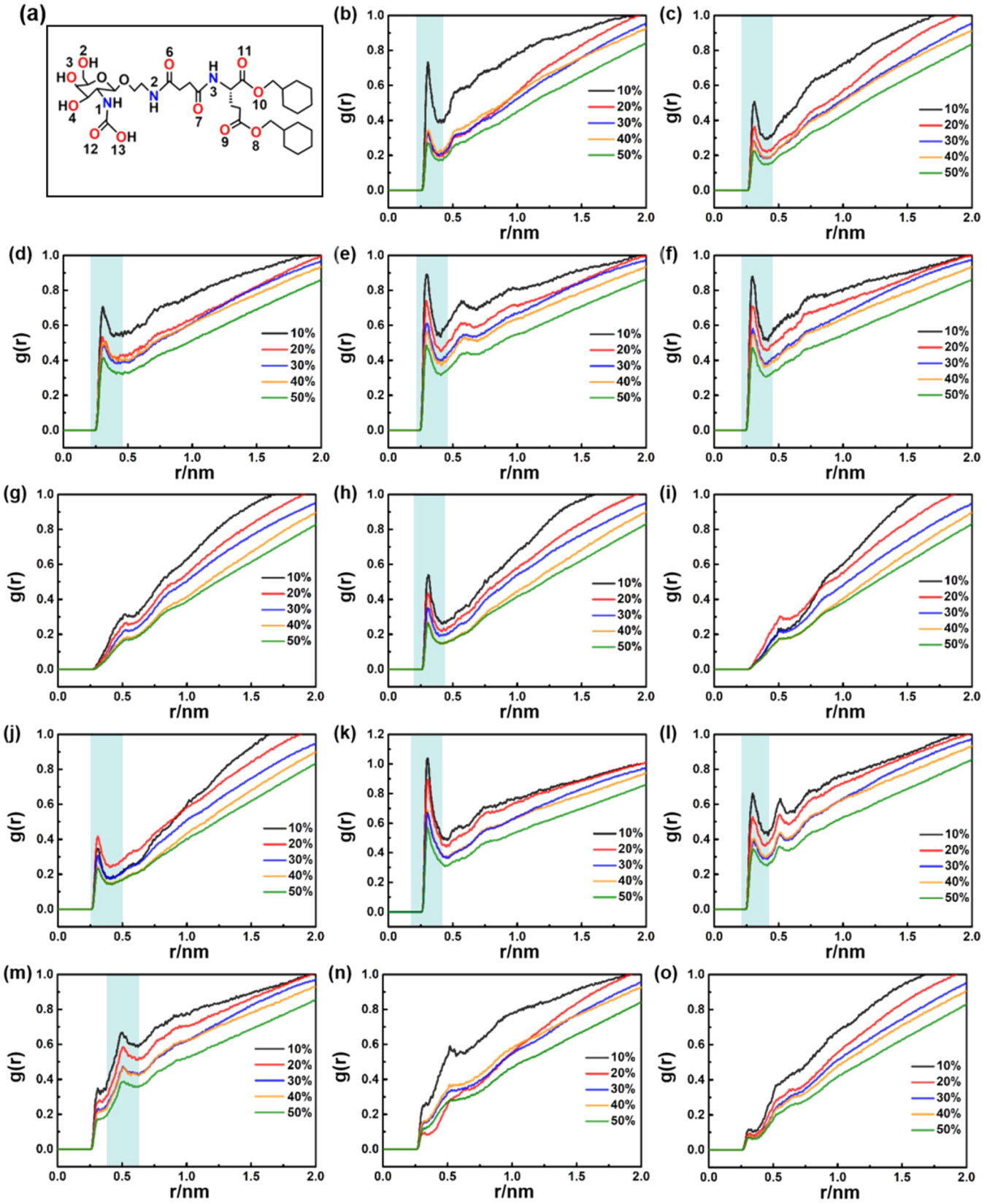

Figure 5. RDF of hydrogels and water. (a) Specific positions of N1, N2, N3, O2, O3, O4, O6, O7, O8, O9, O10, O11, O12, and O13 in the molecule, (b) O6−OW, (c) O7−OW, (d) O2−OW, (e) O3−OW, (f) O4−OW, (g) O8−OW, (h) O9−OW, (i) O10−OW, (j) O11−OW, (k) O12−OW, (l) O13−OW, (m) N1−OW, (n) N2−OW, and (o) N3−OW.

N3) in amide bonds, and oxygen atoms in water molecules (OW). The results are summarized in Figure 5. Figure 5a illustrates the specific positions of the above types of atoms in the molecule. Figure 5b,c shows the RDF results of O6 and O7

https://doi.org/10.1021/acsomega.1c03510
ACS Omega 2021, 6, 21801−21808

in amide bonds with OW. There is also a relatively obvious peak at 0.3 nm, indicating that the nonbonding interactions between O6 and O7 and water molecules are mainly caused by hydrogen bonds. The RDF results of O2, O3, O4, and OW are presented in Figure 5d–f. The sharp peaks appear at about 0.3 nm in all three figures, indicating that hydroxyl groups on gelators have a strong hydrogen bond interaction with water molecules, which is consistent with the previous analysis. The RDF curves of oxygen atoms on the carboxyl group in the hydrogel with water molecules are shown in Figure 5g–l, which can be divided into two categories. Figure 5g–i presents the RDF results of O8–OW and O10–OW, respectively, and no obvious peak appears on the graph, indicating weak nonbonding interaction between them. However, O9, O11, O12, and O13 all have high peaks with OW at about 0.3 nm, which suggests that there is strong hydrogen bonding between them. Figure 5m–o shows the RDF curves of N1–OW, N2–OW, and N3–OW atomic pairs. There is an obvious peak of N1–OW at 0.5 nm, indicating that there is a strong van der Waals effect between them, while there is no obvious peak of N2–OW and N3–OW, demonstrating that the interaction between N2, N3, and water molecules is relatively weak. According to the discussion about Figure 4, the nitrogen atom on the amide bond is more inclined to form intermolecular hydrogen bonds with other hydrogels. On the whole, except the nitrogen atom on the amide bond, most of the other types of atoms interact strongly with water molecules, which also plays an important role in the stability of the gel network structure.

The relaxation time of the hydrogen bond can reflect the strength of the hydrogen bond between each atom in the gel molecule and water molecule. The longer the relaxation time, the stronger the constraint on the water molecules.[35] Relaxation time can be obtained by the autocorrelation function[36]

$$C(t) = \frac{\langle h(t+\tau)h(\tau)\rangle}{\langle h\rangle} \quad (2)$$

In the formula, $h(t)$ is the value of the change of the number of hydrogen bonds. When there is a hydrogen bond between the two atoms, $h(t) = 1$; when there is no hydrogen bond, $h(t) = 0$. According to the results of the RDF, we calculated the autocorrelation functions of hydrogen bonds formed between water molecules and oxygen atoms in hydroxyl oxygen atoms, carboxyl oxygen atoms, and amide bonds and performed exponential fitting on the autocorrelation functions to obtain the relaxation time of hydrogen bonds. As shown in Figure 6, the lifetime autocorrelation function curve of the hydroxyl oxygen atom decays to zero most rapidly with a relaxation time of about 0.77 ps, while the decay curve of the oxygen atom on carboxyl and amide groups basically coincides with each other with a relaxation time of about 2.27 and 2.44 ps, indicating that the stability of the hydrogen bond formed between these types of oxygen atoms and water is stronger than that of the hydroxyl oxygen atom.

In order to study the hydrodynamics of the GalNAc-suc-glu(*O*-methyl-*cyc*-hexyl)$_2$ hydrogel and understand the diffusion of water molecules in the hydrogel network, the mean square displacements(MSDs) of water molecules were analyzed. The MSD is calculated by eq 3[37]

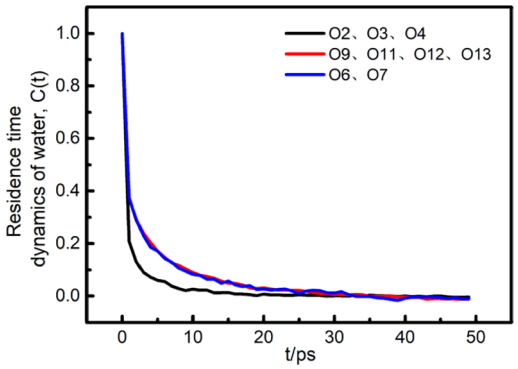

Figure 6. Time correlation function $[C(t)]$ for the hydrogen bonds formed between certain atoms of the hydrogel and water molecules.

$$\mathrm{MSD}(t) = \left\langle \frac{1}{N}\sum_{i=1}^{N}[ri(t) - ri(0)]^2 \right\rangle \quad (3)$$

where N is the number of water molecules, $r_i(t)$ and $r_i(0)$ are the final and initial positions of the water molecular mass center at time t. The angle brackets represent the ensemble average. According to Müller-Plathe,[38] the resulting diffusion mechanism is normal when the slope of log (MSD) and log (t) is close to 1. Figure 7 shows the slopes of log (MSD)–log (t)

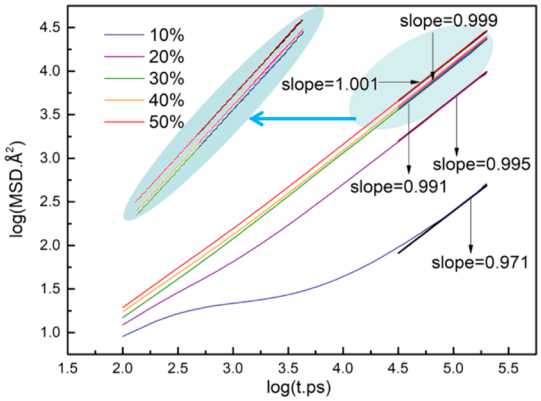

Figure 7. Log (MSD)–log (t) curves for the diffusion of water molecules in hydrogels with various water contents.

of the systems with different water contents (0.971, 0.995, 0.991, 0.999, and 1.001), indicating that the diffusion behavior of the systems is consistent with the law. According to the Einstein equation, the diffusion coefficients (D) are given by the following formula 4[39]

$$D = \frac{1}{2dN}\lim_{t\to\infty}\frac{\mathrm{d}}{\mathrm{d}t}\sum_{i=1}^{N}\langle[ri(t) - ri(0)]^2\rangle \quad (4)$$

The diffusion coefficients of water molecules in different systems are given in Table 1. From the table, with the increase in water content, the diffusion coefficient of water molecules also increases, but all of them are smaller than pure water's self-diffusion in bulk, which is about 5.05×10^{-5} cm^2·s^{-1}. It is proved that hydrogels, after self-assembly, could reduce the diffusion rate of water molecules and restrict the movement of water molecules to some extent. Also, as water content rises, the cross-linking between hydrogels becomes sparse and the

https://doi.org/10.1021/acsomega.1c03510
ACS Omega 2021, 6, 21801–21808

Table 1. Self-Diffusion Coefficients of Water in Different Systems

water content wt %	10	20	30	40	50
diffusion coefficients ($\times 10^{-5}$ $cm^2 \cdot s^{-1}$)	0.0390	0.8134	1.9259	2.0752	2.4732

distance between the molecular chains increases, so the ability to constrain water molecules is weakened.

4. CONCLUSIONS

In summary, we used quantum chemistry calculations and MD methods to simulate the self-assembly of GalNac-suc-glu(*O*-methyl-*cyc*-hexyl)$_2$ into hydrogels in aqueous solution. We constructed systems with different water contents and studied their spontaneous aggregation variation with water. Through the analysis of the number of hydrogen bonds and the RDF, it is found that a large number of hydrogen bonds are formed between hydrogel molecules, and it is the existence of these hydrogen bonds that makes the hydrogel network stable. The interaction between hydrogel molecules and water molecules also exists, and the interaction increases slowly when the water content increases. In addition, the diffusion coefficient of water was also calculated. With the increase in water content, the diffusion coefficient of water also increases gradually because the entry of water molecules causes the gel network structure to expand and promote diffusion. This research method is helpful for us to deeply understand the formation mechanism of hydrogel self-assembly and has guiding significance for the design and development of hydrogels.

■ ASSOCIATED CONTENT

Supporting Information

The Supporting Information is available free of charge at https://pubs.acs.org/doi/10.1021/acsomega.1c03510.

Optimized molecular structure of GalNAc-suc-glu (*O*-methyl-*cyc*-hexyl)$_2$ and energy profile of the system with 50% water content at the final 50 ns of the simulation (PDF)

■ AUTHOR INFORMATION

Corresponding Authors

Heng Zhang − *School of Chemistry and Chemical Engineering, Shandong University, Jinan 250100, China*; Email: zhangheng@sdu.edu.cn

Zhaoyong Guan − *School of Chemistry and Chemical Engineering, Shandong University, Jinan 250100, China*; orcid.org/0000-0002-4103-6507; Email: zyguan666666@qq.com

Yanyan Jiang − *Key Laboratory for Liquid-Solid Structural Evolution and Processing of Materials, Ministry of Education, Shandong University, Jinan 250061, China; Suzhou Institute of Shandong University, Suzhou 215123, China; Shenzhen Research Institute of Shandong University, Shenzhen 518057, China*; orcid.org/0000-0002-7866-4689; Email: yanyan.jiang@sdu.edu.cn

Authors

Yi Zhou − *Key Laboratory for Liquid-Solid Structural Evolution and Processing of Materials, Ministry of Education, Shandong University, Jinan 250061, China*

Jiamei Liu − *Key Laboratory for Liquid-Solid Structural Evolution and Processing of Materials, Ministry of Education, Shandong University, Jinan 250061, China*

Hui Li − *Key Laboratory for Liquid-Solid Structural Evolution and Processing of Materials, Ministry of Education, Shandong University, Jinan 250061, China*; orcid.org/0000-0002-1457-8650

Complete contact information is available at: https://pubs.acs.org/10.1021/acsomega.1c03510

Notes

The authors declare no competing financial interest.

■ ACKNOWLEDGMENTS

The authors would like to acknowledge the support from the National Natural Science Foundation of China (grant no. 11904203), the Shenzhen Fundamental Research Program (JCYJ20190807092803583), the Natural Science Foundation of Jiangsu Province (grant no. BK20190205), the Guangdong Basic and Applied Basic Research Foundation (grant no. 2019A1515110846), and the Fundamental Research Funds of Shandong University (grant no. 2019GN065). The Special Funding also supports this work in the Project of the Taishan Scholar Construction Engineering and Qilu Young Scholar Program of Shandong University. The scientific calculations in this paper were performed on the HPC Cloud Platform of Shandong University.

■ REFERENCES

(1) Li, Y.; Cao, Y. The Physical Chemistry for the Self-assembly of Peptide Hydrogels. *Chin. J. Polym. Sci.* **2017**, *36*, 366−378.

(2) Du, X.; Zhou, J.; Shi, J.; Xu, B. Supramolecular Hydrogelators and Hydrogels: From Soft Matter to Molecular Biomaterials. *Chem. Rev.* **2015**, *115*, 13165−13307.

(3) Jiang, X.; Wang, C.; Han, Q. Molecular dynamic simulation on the state of water in poly(vinyl alcohol) hydrogel. *Comput. Theor. Chem.* **2017**, *1102*, 15−21.

(4) Xing, R.; Zou, Q.; Yan, X. Peptide-based Supramolecular Colloids. *Acta Phys.-Chim. Sin.* **2020**, *36*, 1909048.

(5) Komatsu, H.; Ikeda, M.; Hamachi, I. Mechanical Reinforcement of Supramolecular Hydrogel through Incorporation of Multiple Noncovalent Interactions. *Chem. Lett.* **2011**, *40*, 198−200.

(6) Jiao, J.; Xu, G.; Xin, X. Effect of Bile Salts on Self-Assembly and Construction of Micro-/nanomaterials. *Acta Phys.-Chim. Sin.* **2019**, *35*, 684−696.

(7) Shigemitsu, H.; Hamachi, I. Supramolecular Assemblies Responsive to Biomolecules toward Biological Applications. *Chem.—Asian J.* **2015**, *10*, 2026−2038.

(8) Sun, T.-Y.; Liang, L.-J.; Wang, Q.; Laaksonen, A.; Wu, T. A molecular dynamics study on pH response of protein adsorbed on peptide-modified polyvinyl alcohol hydrogel. *Biomater. Sci.* **2014**, *2*, 419−426.

(9) Snigdha, K.; Singh, B. K.; Mehta, A. S.; Tewari, R. P.; Dutta, P. K. Self-assembling N -(9-Fluorenylmethoxycarbonyl)-l-Phenylalanine hydrogel as novel drug carrier. *Int. J. Biol. Macromol.* **2016**, *93*, 1639−1646.

(10) Qi, J.; Yan, Y.; Cheng, B.; Deng, L.; Shao, Z.; Sun, Z.; Li, X. Enzymatic Formation of an Injectable Hydrogel from a Glycopeptide as a Biomimetic Scaffold for Vascularization. *ACS Appl. Mater. Interfaces* **2018**, *10*, 6180−6189.

(11) Zou, P.; Chen, W.-T.; Sun, T.; Gao, Y.; Li, L.-L.; Wang, H. Recent advances: peptides and self-assembled peptide-nanosystems for antimicrobial therapy and diagnosis. *Biomater. Sci.* **2020**, *8*, 4975−4996.

(12) Kiyonaka, S.; Shinkai, S.; Hamachi, I. Combinatorial library of low molecular-weight organo- and hydrogelators based on glycosylated amino acid derivatives by solid-phase synthesis. *Chem.—Eur. J.* **2003**, *9*, 976−983.
(13) Shigemitsu, H.; Hamachi, I. Design Strategies of Stimuli-Responsive Supramolecular Hydrogels Relying on Structural Analyses and Cell-Mimicking Approaches. *Acc. Chem. Res.* **2017**, *50*, 740−750.
(14) Matsumoto, S.; Yamaguchi, S.; Wada, A.; Matsui, T.; Ikeda, M.; Hamachi, I. Photo-responsive gel droplet as a nano- or pico-litre container comprising a supramolecular hydrogel. *Chem. Commun.* **2008**, *13*, 1545−1547.
(15) Angelerou, M. G. F.; Frederix, P. W. J. M.; Wallace, M.; Yang, B.; Rodger, A.; Adams, D. J.; Marlow, M.; Zelzer, M. Supramolecular Nucleoside-Based Gel: Molecular Dynamics Simulation and Characterization of Its Nanoarchitecture and Self-Assembly Mechanism. *Langmuir* **2018**, *34*, 6912−6921.
(16) Bertran, O.; Saldías, C.; Díaz, D. D.; Alemán, C. Molecular dynamics simulations on self-healing behavior of ionene polymer-based nanostructured hydrogels. *Polymer* **2020**, *211*, 123072.
(17) Hou, D.; Xu, J.; Zhang, Y.; Sun, G. Insights into the molecular structure and reinforcement mechanism of the hydrogel-cement nanocomposite: An experimental and molecular dynamics study. *Composites, Part B* **2019**, *177*, 107421.
(18) Manandhar, A.; Kang, M.; Chakraborty, K.; Tang, P. K.; Loverde, S. M. Molecular simulations of peptide amphiphiles. *Org. Biomol. Chem.* **2017**, *15*, 7993−8005.
(19) Delley, B. An all-electron numerical method for solving the local density functional for polyatomic molecules. *J. Chem. Phys.* **1990**, *92*, 508−517.
(20) Delley, B. From Molecules to Solids with the Dmol3 Approach. *J. Chem. Phys.* **2000**, *113*, 7756−7764.
(21) Perdew, J. P.; Burke, K.; Ernzerhof, M. Generalized Gradient Approximation Made Simple. *Phys. Rev. Lett.* **1996**, *77*, 3865−3868.
(22) Grimme, S. Density functional theory with London dispersion corrections. *Wiley Interdiscip. Rev.: Comput. Mol. Sci.* **2011**, *1*, 211−228.
(23) Hashemnejad, S. M.; Huda, M. M.; Rai, N.; Kundu, S. Molecular Insights into Gelation of Di-Fmoc-l-Lysine in Organic Solvent-Water Mixtures. *ACS Omega* **2017**, *2*, 1864−1874.
(24) Huda, M. M.; Rai, N. Probing Early-Stage Aggregation of Low Molecular Weight Gelator in an Organic Solvent. *J. Phys. Chem. B* **2020**, *124*, 2277−2288.
(25) Marrink, S. J.; Risselada, H. J.; Yefimov, S.; Tieleman, D. P.; de Vries, A. H.; Alex, H. The MARTINI Force Field: Coarse Grained Model for Biomolecular Simulations. *J. Phys. Chem. B* **2007**, *111*, 7812−7824.
(26) Malde, A. K.; Zuo, L.; Breeze, M.; Stroet, M.; Poger, D.; Nair, P. C.; Oostenbrink, C.; Mark, A. E. An Automated Force Field Topology Builder (ATB) and Repository: Version 1.0. *J. Chem. Theory Comput.* **2011**, *7*, 4026−4037.
(27) Hess, B.; Kutzner, C.; van der Spoel, D.; Lindahl, E. GROMACS 4: Algorithms for Highly Efficient, Load-Balanced, and Scalable Molecular Simulation. *J. Chem. Theory Comput.* **2008**, *4*, 435−447.
(28) Humphrey, W.; Dalke, A.; Schulten, K. VMD: visual molecular dynamics. *J. Mol. Graphics* **1996**, *14*, 33−38.
(29) Nguyen, H. D. Self-Assembly of Stimuli-Responsive Hydrogel Nanostructures by Peptide Amphiphiles via Molecular Dynamics Simulations. *Biophys. J.* **2014**, *106*, 420a.
(30) Hamachi, I.; Kiyonaka, S.; Shinkai, S. Solid-phase lipid synthesis (SPLS)-2: incidental discovery of organogelators based on artificial glycolipids. *Tetrahedron Lett.* **2001**, *42*, 6141−6145.
(31) Kiyonaka, S.; Shinkai, S.; Hamachi, I. Combinatorial Library of Low Molecular-Weight Organo- and Hydrogelators Based on Glycosylated Amino Acid Derivatives by Solid-Phase Synthesis. *Chem.—Eur. J.* **2003**, *9*, 976−983.
(32) Luzar, A.; Chandler, D. Structure and hydrogen bond dynamics of water-dimethyl sulfoxide mixtures by computer simulations. *J. Chem. Phys.* **1993**, *98*, 8160.
(33) Chen, Z. L.; Xu, W. R.; Tang, L. D. *The Theory and Application of Molecular Simulation*; Chemical Industry Press: Beijing, 2007.
(34) Wang, Y.-e.; Wei, Q.-h.; Yang, M.-m.; Wei, S.-m. Molecular dynamics simulation on mechanical properties of PVP/PVA. *J. Med. Biomech.* **2014**, *29*, E99−E104.
(35) Guo, K.; Zhang, H.; Sun, J.; Yuan, S.; Liu, C. Molecular Dynamics Simulation on Self-Assembly of Fmoc-FF Dipeptide. *Chem. J. Chin. Univ.* **2015**, *36*, 2171−2178.
(36) Lopez, C. F.; Nielsen, S. O.; Klein, M. L.; Moore, P. B. Hydrogen Bonding Structure and Dynamics of Water at the Dimyristoylphosphatidylcholine Lipid Bilayer Surface from a Molecular Dynamics Simulation. *J. Phys. Chem. B* **2004**, *108*, 6603−6610.
(37) Zhang, H.; Wang, H.; Xu, G.; Yuan, S. A molecular dynamics simulation of N-(fluorenyl-9-methoxycarbonyl)-dipeptides supramolecular hydrogel. *Colloids Surf., A* **2013**, *417*, 217−223.
(38) Müller-Plathe, F. Permeation of polymers-a computational approach. *Acta Polym.* **1994**, *45*, 259−293.
(39) Tamai, Y.; Tanaka, H.; Nakanishi, K. Molecular Dynamics Study of Polymer−Water Interaction in Hydrogels. 2. Hydrogen-Bond Dynamics. *Macromolecules* **1996**, *29*, 6761−6769.

https://doi.org/10.1021/acsomega.1c03510
ACS Omega 2021, 6, 21801−21808